applied sciences

MDPI

Article

Prediction of Leakage Flow Rate and Blow-Down in Brush Seals via 2D CFD Simulation with Porosity Correction

Jeong Woo Kwon [1] and Joon Ahn [2,*]

[1] Department of Mechanical Engineering, Graduate School, Kookmin University, 77 Jeongneung-ro, Seongbuk-gu, Seoul 02707, Republic of Korea
[2] School of Mechanical Engineering, Kookmin University, 77 Jeongneung-ro, Seongbuk-gu, Seoul 02707, Republic of Korea
* Correspondence: jahn@kookmin.ac.kr

Abstract: Brush seals are extensively used in rotating equipment, such as gas turbines and compressors, providing effective sealing while accommodating radial, axial, and angular movements between components. In this study, the performance of brush seals with and without clearances was predicted through axisymmetric 2D computational fluid dynamic (CFD) simulations using a porous media model. Because the accurate modeling of a brush seal requires the appropriate porosity to be determined and the flow resistance to be calculated, a porosity correction was performed based on the brush seal's geometry and pressure ratio. The corrected porosity was then used to calculate the flow resistance and the leakage flow rate was predicted. Based on the results, the corrected porosity significantly improved the accuracy of the previously unreliable leakage flow rate predictions, regardless of the presence of clearances. For cases with a clearance, the blow-down effect was determined through CFD simulations for the given geometry and was compared with experimental data. The leakage flow rate predictions were highly accurate, with a relative error of less than 5% across a pressure ratio range of 1.5–4.

Keywords: brush seal; porosity correction factor; flow resistance; leakage flow rate; blow-down

Citation: Kwon, J.W.; Ahn, J. Prediction of Leakage Flow Rate and Blow-Down in Brush Seals via 2D CFD Simulation with Porosity Correction. *Appl. Sci.* **2024**, *14*, 8821. https://doi.org/10.3390/app14198821

Academic Editor: Mark J. Jackson

Received: 26 August 2024
Revised: 25 September 2024
Accepted: 28 September 2024
Published: 30 September 2024

1. Introduction

A gas turbine is a fluid machine designed based on the Brayton cycle, and is primarily used as an engine for generators or propulsion systems, therefore, its efficiency is a critical factor affecting its performance. The efficiency of a gas turbine can be improved through various methods, but the most effective approach is to increase the turbine inlet temperature, which enhances the cycle efficiency [1]. However, material limitations impose constraints on raising the turbine inlet temperature. To overcome these constraints, cooling techniques are employed to supply cooling fluid to both the interior and exterior of the turbine blades. However, the cooling fluid is delivered to the blades through secondary flow paths [2,3], where gaps inevitably form between rotating and stationary components to enable rotation. These gaps can lead to leakage of the cooling fluid, necessitating appropriate sealing measures.

Labyrinth seals have been widely used in sealing applications, however, in recent years, flexible and durable brush seals have been increasingly adopted. Compared with traditional labyrinth seals, brush seals can reduce leakage by up to 80% [4] and are better equipped to handle the temperature and pressure fluctuations that occur under high-temperature and high-pressure operating conditions. Thus, brush seals significantly contribute to improving the performance and lifespan of turbines [5] and are now commonly used in modern gas turbines [6]. In aerospace applications, brush seals offer distinct advantages over traditional sealing methods, particularly because of their ability to reduce leakage by up to 50%, which directly improves engine efficiency and reduces fuel consumption. Their design allows them to maintain tight clearances, even under challenging conditions

such as thermal variations and stop/start operation, where traditional labyrinth seals tend to degrade. Their durability and consistent performance render brush seals especially valuable in modern aerospace engines, where precise clearance control is essential for optimizing propulsion and minimizing energy losses [7].

As shown in Figure 1, a brush seal consists of three primary components: the bristle pack, the front plate, and the backing plate. The bristle pack, which is composed of fine wires, is fixed at an angle between the front plate and the backing plate. Positioned above the surface of the rotor, the brush seal prevents leakage flow from the high-pressure side to the low-pressure side. The backing plate supports the bristle pack in withstanding pressure loads and prevents small-diameter bristles from escaping outward [8]. As shown in Figure 1a, the fence height refers to the radial distance between the back plate bore and the bristle bore. It plays a key role in determining the pressure limit of a brush seal; a greater fence height reduces the pressure limit due to increased stress on the bristles [9]. The bristles in the brush seal form a flexible barrier between the high-pressure (upstream) and low-pressure (downstream) regions by making contact with the rotor. The front plate ensures the bristle pack's stiffness, while the back plate counters pressure forces [10]. To minimize wear and allow the bristles to adjust to the rotor movement, they are inclined at an angle, known as the lay angle (ϕ), of 30° to 60° with respect to the radial direction, as depicted in Figure 1b [11].

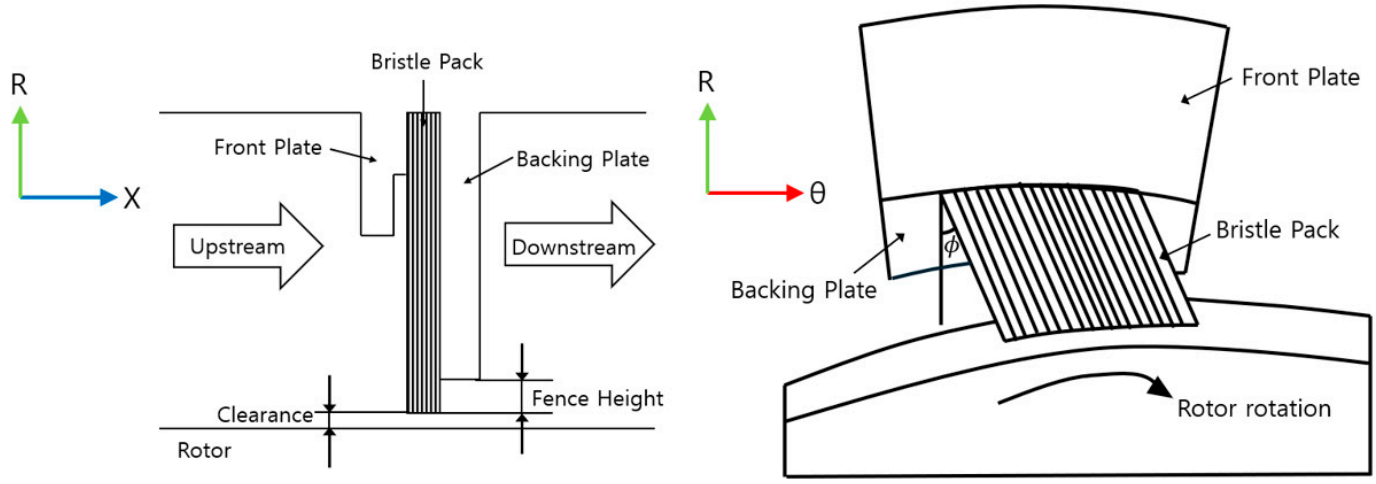

(**a**) (**b**)

Figure 1. (**a**) Cross-section and geometric parameters of brush seal used in turbine rotor. (**b**) Lay angle of brush seal applied to rotor.

The performance characteristics of brush seals under varying flow conditions and different geometric configurations have been primarily investigated through experiments. Neef et al. [12] reported that the initial wear of brush seals varies significantly, depending on the operating conditions. Additionally, they confirmed that brush seals can adapt to a range of operating conditions while maintaining stable performance over time. Pekris et al. [13] demonstrated that the performance of brush seals is influenced by mechanical strength and thermal stability. Based on experimental data, they proposed design improvements such as passive pressure balance and active pressure balance to optimize brush seal performance. However, conducting experiments on brush seals under high-temperature and high-pressure conditions to replicate realistic gas turbine environments poses significant challenges. Consequently, computational fluid dynamics (CFD) is being actively considered as a viable approach for evaluating the performance of brush seals in actual turbine environments [14].

The bristle pack of a brush seal comprises fine wires, thus, performing detailed 3D computer simulations that include each of these wires requires substantial time and resources. Therefore, 2D CFD simulations, in which the bristle pack is modeled as a porous medium, have been widely adopted [15,16]. Due to the axisymmetric structure of the brush seal, its geometry can be simplified to a 2D axisymmetric configuration, which enables efficient computation; in this regard, studies have presented results that closely match experimental leakage flow rates [17]. Specifically, 2D CFD is effective at reducing time and cost during early design stages, which involve numerous design degrees of freedom and variables. However, to capture the 3D effects of actual brush seals and the influence of various components during the analysis process, empirical correlations remain essential.

Clearance is a key geometric parameter that must be carefully considered when designing brush seals. Based on the presence or absence of clearance, brush seals are generally categorized into two types, namely contact seals without clearance and seals with an initial clearance, depending on the requirements for the gas turbine. Most brush seals are designed in a contact configuration, where the bristles interfere with the rotor surface to minimize fluid leakage [18]. Brush seals with an initial clearance are also designed to regulate cooling and leakage flows [19]. This design considers the blow-down effect, where a pressure differential causes the bristles to move radially toward the rotor, thereby gradually reducing the clearance [20]. The blow-down effect occurs when a pressure load is applied to the brush seal, causing the bristles to deflect axially downstream, pivot around the bristle root, and compact against the backing plate surface. Additionally, the incoming flow exerts a bending moment on the bristles due to their lay angle, causing them to bend toward the rotor surface and close the clearance [21]. The clearance between the bristle pack tip and the rotor must be sufficiently large to avoid collision, but an excessive clearance will lead to increased leakage flow [22].

In cases without clearance, the leakage flow rate has been accurately predicted using the Flo-master commercial 1D code, closely matching experimental results [23,24]. However, since most brush seal models in 1D codes, including Flo-master, assume a contact state without clearance, predicting the performance of brush seals with clearance is challenging [24]. In this study, a three-step 2D CFD analysis was conducted to design brush seals with clearance.

In the first step, a 2D CFD simulation was conducted for brush seals without clearance, and the resulting leakage flow rate was compared with experimental data. The simulations were performed for two geometries: those used by Bayley et al. [25] and Carlile et al. [26]. As in previous studies [4,5], the bristle pack was modeled as a porous medium in the CFD calculations, and the porosity and flow resistance values were calibrated to match the experimentally measured leakage flow rates. Through this approach, a porosity correction factor model was developed based on the experimental data.

In the second step, the performance of brush seals with clearances was predicted via 2D CFD simulations. The simulations were conducted based on the geometry presented by Turner et al. [27], which includes clearance. Moreover, the blow-down effect was considered to ensure accurate performance predictions [28]. The porosity correction developed in the previous step for brush seals without clearance was applied, and the leakage flow rate was predicted across different pressure ratios and compared with experimental results.

In cases with clearance, fluid–structure interaction (FSI) analysis is required to simulate the actual movement of the bristle pack, including the blow-down effect [29]. However, dynamic changes in porosity cannot be fully accounted for [30]. Therefore, in the third step, a design formula was developed using 2D CFD to predict the blow-down effect. This formula was designed to be applicable within the parameter range presented by Turner et al. [27], and its effectiveness in predicting leakage flow rates in brush seals with clearance was validated. This study is expected to contribute significantly to brush seal design as it provides a method to accurately predict leakage flow rates with and without clearance.

2. Numerical Method and Validation

The numerical analysis was conducted using the ANSYS Fluent 2021 R1 commercial software program. Flow analysis of the brush seal requires the bristle pack to be modeled. However, analyzing each bristle element individually is impractical as it would require excessive computational resources. Therefore, the bristle pack was modeled using the Porous Media model provided by ANSYS Fluent. However, the porous media approach does not account for 3D effects, hence, since the geometry is axisymmetric, an axisymmetric 2D CFD analysis was conducted. This significantly reduced the computation time, enabling the examination of various geometric parameters and flow conditions.

ANSYS Fluent has been validated extensively in the context of fluid flow analysis and is commonly used for brush seal modeling [31]. The porous media model, frequently employed in brush seal studies, effectively approximates the flow resistance of the bristle pack while maintaining computational efficiency [32]. Although 2D axisymmetric CFD analysis simplifies the problem, studies have shown that it can produce results closely aligned with experimental data for similar applications [33]. The 2D geometry was created as the computational domain, and the mesh was generated using ANSYS Meshing. The mesh for the brush seal was designed with reference to the model created by Germen [34]. Mesh generation was performed using the MultiZone Quad/Tri method to produce a structured mesh. Germen [34] emphasized that the flow behavior within a brush seal is highly complex, requiring dense mesh placement near the walls, within the bristle pack, and in the fence height region to achieve accurate results. In this study, the minimum element size in the fence height region was set to 0.0254 mm for mesh generation [35].

Simulations were conducted for three brush seal geometries: those used by Bayley et al. [25], Carlile et al. [26], and Turner et al. [27]. Among these, the first [25] and second [26] represent brush seals in a contact state without clearance, while the third [27] includes clearance and requires consideration of the blow-down effect. Figure 2 shows the mesh configurations for each of the three geometries. Figure 2b and Table 1 describe the element-sizing method for the three brush seal meshes, with all elements shaped as quadrilaterals. To simplify the calculations, regions other than the fluid flow paths and the bristle pack were excluded from the computational domain. In the bristle pack region, fluid velocity decreases, leading to laminar flow. Therefore, a laminar model was applied to the bristle pack section [36].

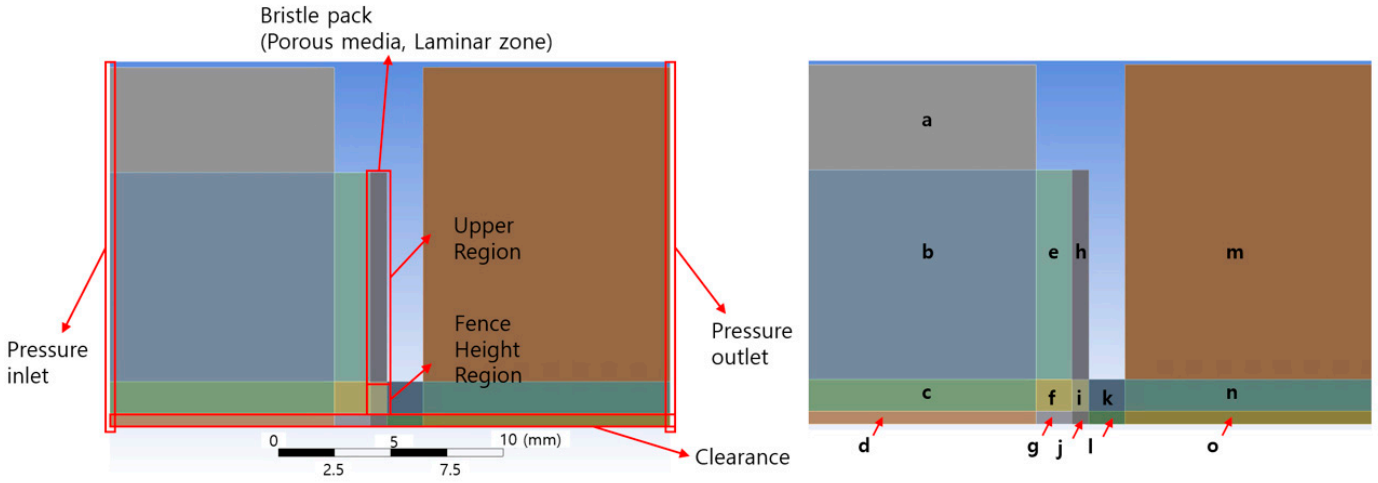

(**a**) (**b**)

Figure 2. *Cont.*

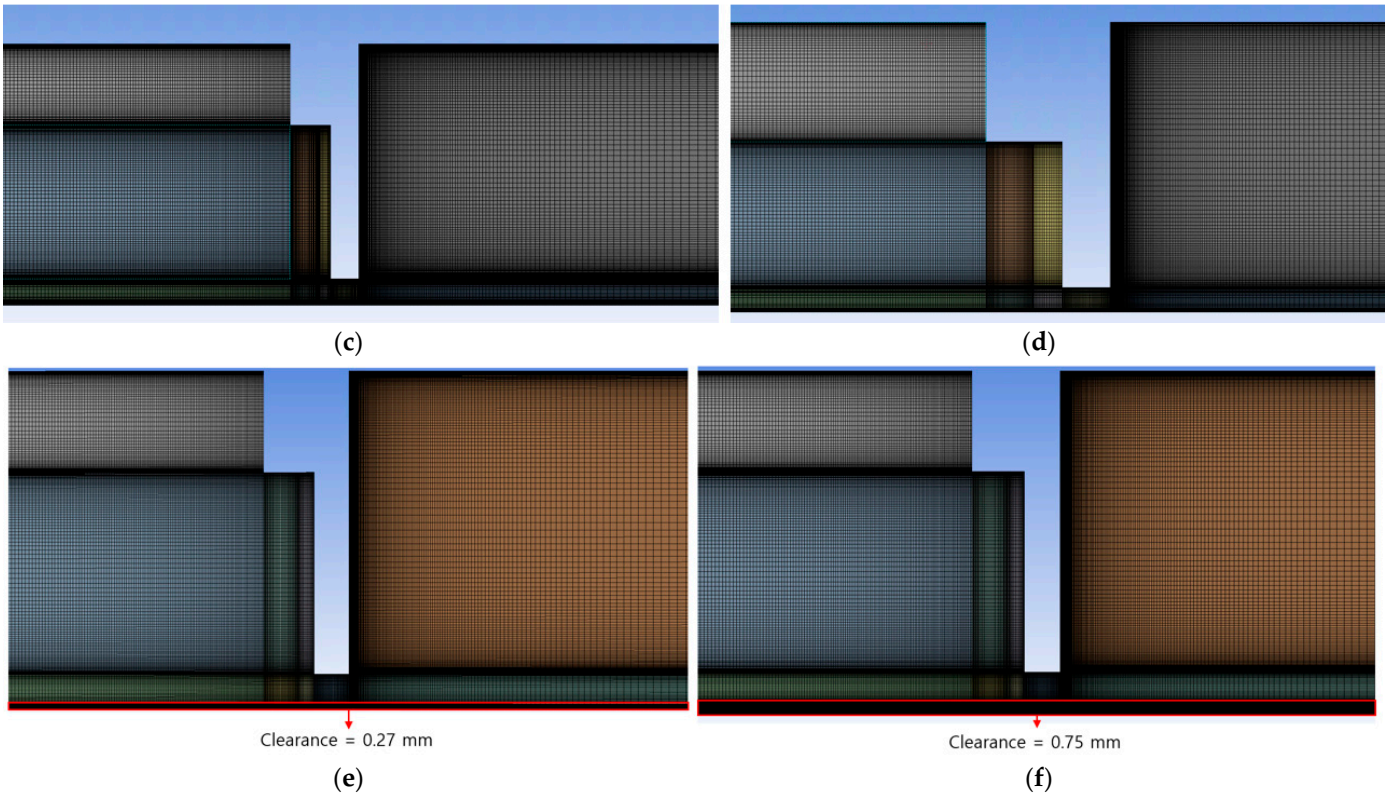

Figure 2. (**a**) Computational domain and boundary conditions including porous medium model grid systems; (**b**) labeled meshes for brush seals without clearance used by (**c**) Bayley et al. [25] and (**d**) Carlile et al. [26], and for brush seals used by Turner et al. [27] with (**e**) clearance = 0.27 mm and (**f**) clearance = 0.75 mm.

Table 1. Element-sizing method for each labeled mesh.

Label	Maximum Element Size (mm)	Minimum Element Size (mm)	Boundary Condition	Material	Geometry
a	0.5	0.04	Pressure_inlet	Fluid	Left edge
b	0.48	0.038	Pressure_inlet	Fluid	Left edge
c	0.45	0.035	Pressure_inlet	Fluid	Left edge
d	0.25	0.015	Pressure_inlet	Fluid	Left edge
e	0.52	0.042	-	Fluid	-
f	0.4	0.032	-	Fluid	-
g	0.25	0.015	-	Fluid	-
h	0.47	0.039	Bristle_Upper	Porous medium	Body
i	0.45	0.035	Bristle_FenceHeight	Porous medium	Body
j	0.3	0.02	-	Fluid	-
k	0.31	0.0254	-	Fluid	-
l	0.3	0.02	-	Fluid	-
m	0.45	0.035	Pressure_outlet	Fluid	Right edge
n	0.45	0.035	Pressure_outlet	Fluid	Right edge
o	0.3	0.02	Pressure_outlet	Fluid	Right edge

The most widely used models for the flow analysis of brush seals are the k–ε and k–ω SST turbulence models [37,38]. In this study, these two turbulence models were compared based on the brush seal geometry used by Bayley et al. [25]. The leakage flow rate of the brush seal was used as the evaluation metric, and the results are presented in Figure 3. In

ANSYS Fluent, the leakage flow rate was calculated at the pressure boundary inlet using Equation (1):

$$\dot{m} = \int_A \rho \cdot \vec{u} \cdot dA. \quad (1)$$

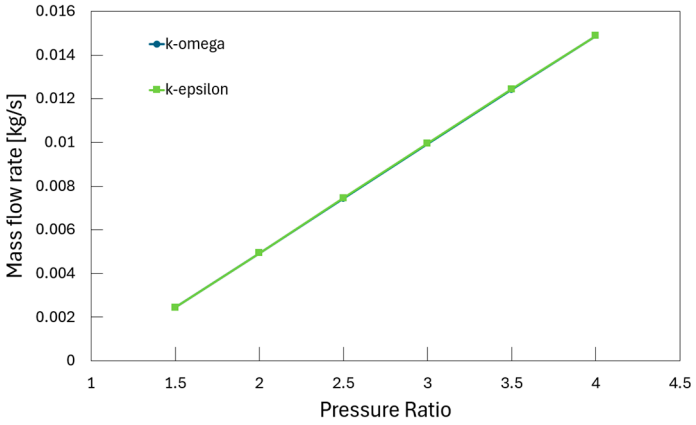

Figure 3. Leakage flow rate in brush seal without clearance [25] according to turbulence model.

As shown in Figure 3, the difference in the predicted leakage flow rate between the two models was minimal. However, the k–ε model was selected for analyzing the flow field of the brush seal. This model is known to provide accurate predictions for high-Reynolds-number flows under high-pressure and high-speed operating conditions [35], and it has also been reported to yield reliable results when pressure boundary conditions are applied at the inlet and outlet [39]. Therefore, the realizable k–ε model, which is commonly used for brush seals, was adopted in this study, and enhanced wall treatment was applied to predict the near-wall flow more accurately [40]. Brush seals, which consist of densely packed bristles near rotating components, are particularly sensitive to wall effects on fluid flow. Enhanced wall treatment is a robust approach that combines low–Reynolds number models for resolving the near-wall region and wall functions for regions farther from the wall. This combination ensures a smooth transition between the viscosity-affected near-wall region and the fully turbulent outer region [41]. The mesh configurations presented in Figure 2 were designed to ensure that y + <5, which is required for applying enhanced wall treatment [42].

A grid-sensitivity test was conducted, the results of which are presented in Figure 4. The criterion for grid independence was determined by selecting the mesh size that resulted in a <0.2% error in leakage flow rate for all three geometries [25–27,43]. For the Bayley et al. [25] geometry, grid independence was achieved with a mesh count of 62,750 or more; to minimize the error in leakage flow rate, 78,783 elements were selected. For the Carlile et al. [26] geometry, grid independence was confirmed at 113,340 elements, and the simulations were performed with 146,025 elements. For the Turner et al. [27] geometry, with a 0.27 mm clearance, grid independence was achieved with 90,762 elements, and 110,020 elements were selected for the final simulations.

The porosity of the bristle pack in the brush seal was calculated for the three geometries [25–27] using the formula developed by Chew et al. [44]:

$$\varepsilon = 1 - \frac{\pi d^2 N}{4 t sin\phi}. \quad (2)$$

The porosity calculated using Equation (2) was then used to determine the flow resistance of the porous media, as expressed in Equation (3), an empirical formula developed by Pröstler [45], who refined Chew et al.'s model [44] based on experimental data. The flow resistance values were utilized in the CFD simulations as part of the porous media model to simulate the pressure drop and flow distribution through the bristle pack. Pröstler's

formula [45] has been proven effective in calculating the stiffness and damping coefficients of brush seals, as referenced by Pugachev et al. [46].

$$a_n = 80C,\ a_s = 32\varepsilon C,\ C = \frac{(1-\varepsilon)^2}{\varepsilon^3 d^2} \tag{3}$$

$$b_n = 1.16D,\ b_s = 0,\ D = \frac{1-\varepsilon}{\varepsilon^3 d}.$$

To ensure a closer match with the experimental data, the bristle pack was divided into two regions: the fence height region and the upper region. According to Dogu [5], for consistency with experimental results, the flow resistance in the upper region should be set 20% higher than that in the fence height region. Therefore, the flow resistance calculated using Equation (3) was applied to the fence height region, while a 20% higher flow resistance was used for the upper region.

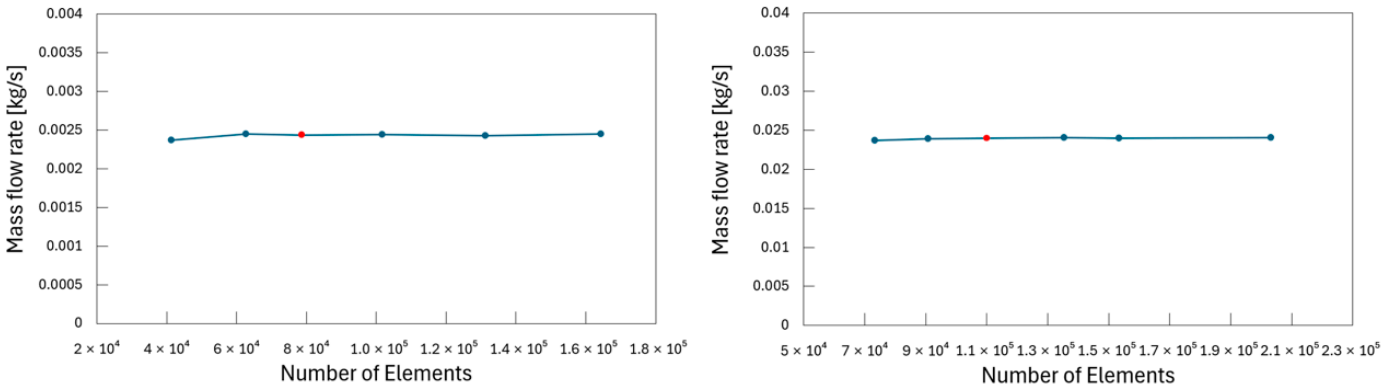

(**a**) (**b**)

Figure 4. Grid-sensitivity test results: (**a**) brush seal without clearance (Bayley et al. [25]); (**b**) brush seal with clearance (Turner et al. [27], clearance = 0.27 mm).

3. Results and Discussion

3.1. Porosity Correction Factor

When CFD simulations were conducted using the flow resistance obtained from Equation (3) based on the porosity calculated using Equation (2), a significant discrepancy was observed with respect to the experimental results. As shown in Figure 5, the CFD-predicted leakage flow rate was underestimated relative to the experimental data of Bayley et al. [25]. Notably, a significant error was observed, with the maximum relative error reaching approximately 50% in the section with a pressure ratio of 2.75. Therefore, we established a formula for a porosity correction factor that could be utilized in CFD calculations for each brush seal geometry. Equation (4) considers variables such as bristle pack thickness [40], bristle diameter [47], and fence height [48], which are key factors affecting the flow in brush seals. This formula is designed under the assumptions that the porosity of the bristle pack decreases as the pressure ratio increases [47], and that if a clearance is present, the blow-down effect reduces the bristle porosity further [49]. The correction factor calculated using Equation (3) is multiplied by the porosity obtained from Equation (2). Equation (3) is applicable within a pressure ratio range of 1.5–6, and it provides predictions with a coefficient of determination (R^2) of 0.98 or higher.

$$\alpha = 0.4581 \cdot PR^{-0.0789} \cdot \left(\frac{H}{d}\right)^{0.8468} \cdot \left(\frac{t}{d}\right)^{-0.6604} - 0.2686 \cdot \left(\frac{CL}{d}\right)^{0.5297} \tag{4}$$

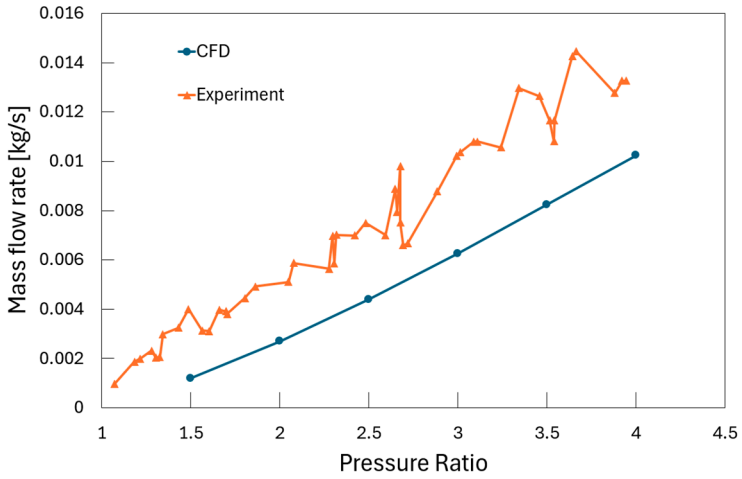

Figure 5. Leakage flow rate predicted based on 2D CFD simulation with porosity obtained from the initial geometry used by Bayley et al. [25].

3.2. Simulation of Contact Brush Seal with Porosity Correction

For brush seals in a contact state without clearance, the geometries used by Bayley et al. [25] and Carlile et al. [26] were analyzed via 2D CFD simulation. The geometrical parameters and flow conditions are listed in Table 2. Figure 6 compares the CFD results with the experimental data. The main differences between the two brush seal geometries lie in their bristle diameter, bristle pack thickness, and bristle density. These differences significantly affect the porosity of each brush seal, leading to variations in flow characteristics and performance. Additionally, as the fence height differs by more than two-fold between these geometries, analyzing the associated difference in flow behavior is crucial.

Table 2. Flow conditions and geometrical parameters of brush seals without clearance [25,26].

Parameter	Bayley et al. [25]	Carlile et al. [26]
Bristle diameter (d)	0.0762 mm	0.051 mm
Bristle pack thickness (t)	0.7 mm	0.8 mm
Bristle lay angle (ϕ)	45°	40°
Fence height (H)	1.5 mm	0.655 mm
Clearance (CL)	0 mm	0 mm
Bristle density (N)	94.5 per mm	180 per mm
Upstream temperature	293.15 K	290 K
Downstream pressure	100 kPa	100 kPa
Pressure patio $\left(\frac{p_u}{p_d}\right)$	1.07–3.8	2–8
Porosity (ε)	0.129	0.285

As shown in Figure 6a, the leakage flow rates were accurately predicted for the two geometries. However, as seen in Figure 6b, the predictions were less accurate for pressure ratios above 6; this is attributed to the increasing influence of the non-linear effects arising from the combination of high pressure and friction in the brush seals [50].

For both the Bayley et al. [25] and Carlile et al. [26] geometries, the pressure (Figure 7a) was the highest upstream and gradually decreased as the fluid passed through the bristle pack toward the downstream region. For the Bayley et al. [25] geometry, the pressure drop occurred gradually through the bristle pack, enabling a more stable state to be maintained downstream. However, for the Carlile et al. [26] geometry, the pressure decreased more rapidly and stabilized relatively quickly in the downstream region.

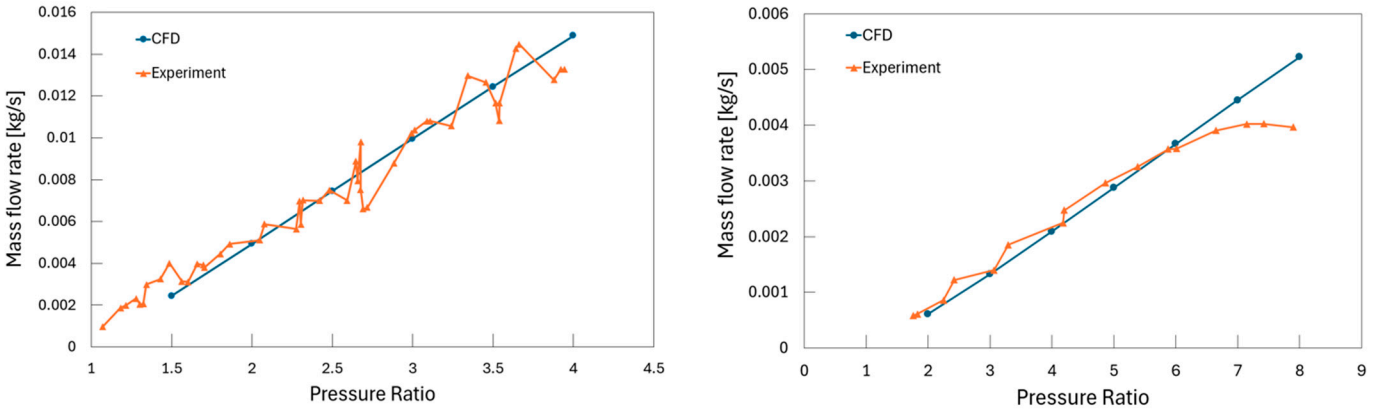

(**a**) (**b**)

Figure 6. Leakage flow rates of contact brush seals predicted by 2D CFD with porosity correction: (**a**) Bayley et al. [25]; (**b**) Carlile et al. [26].

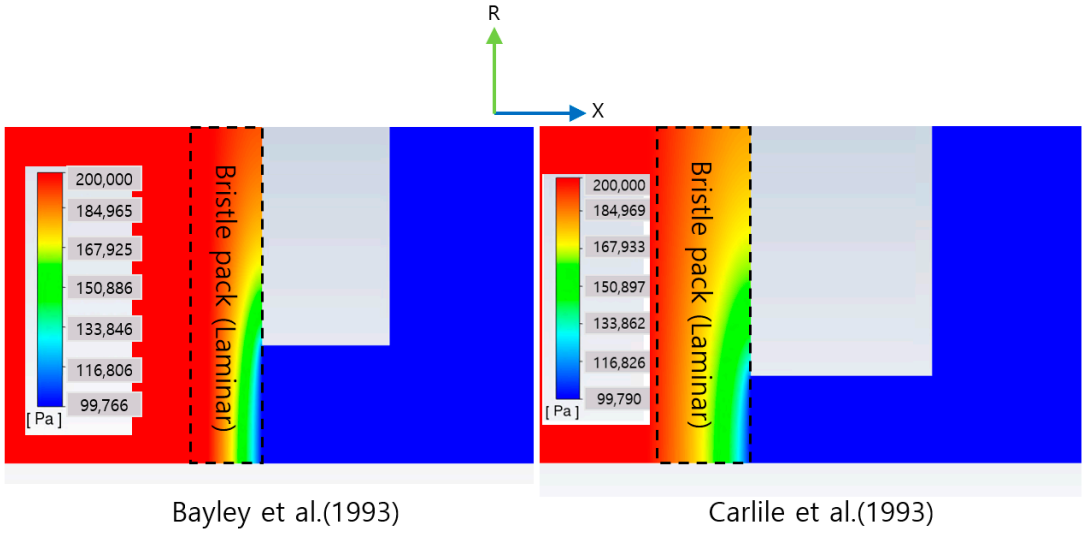

(**a**)

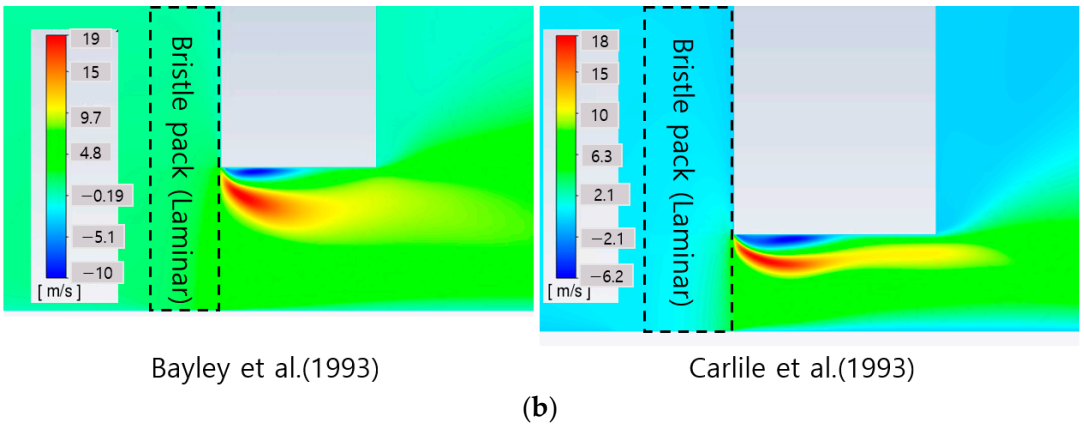

(**b**)

Figure 7. *Cont.*

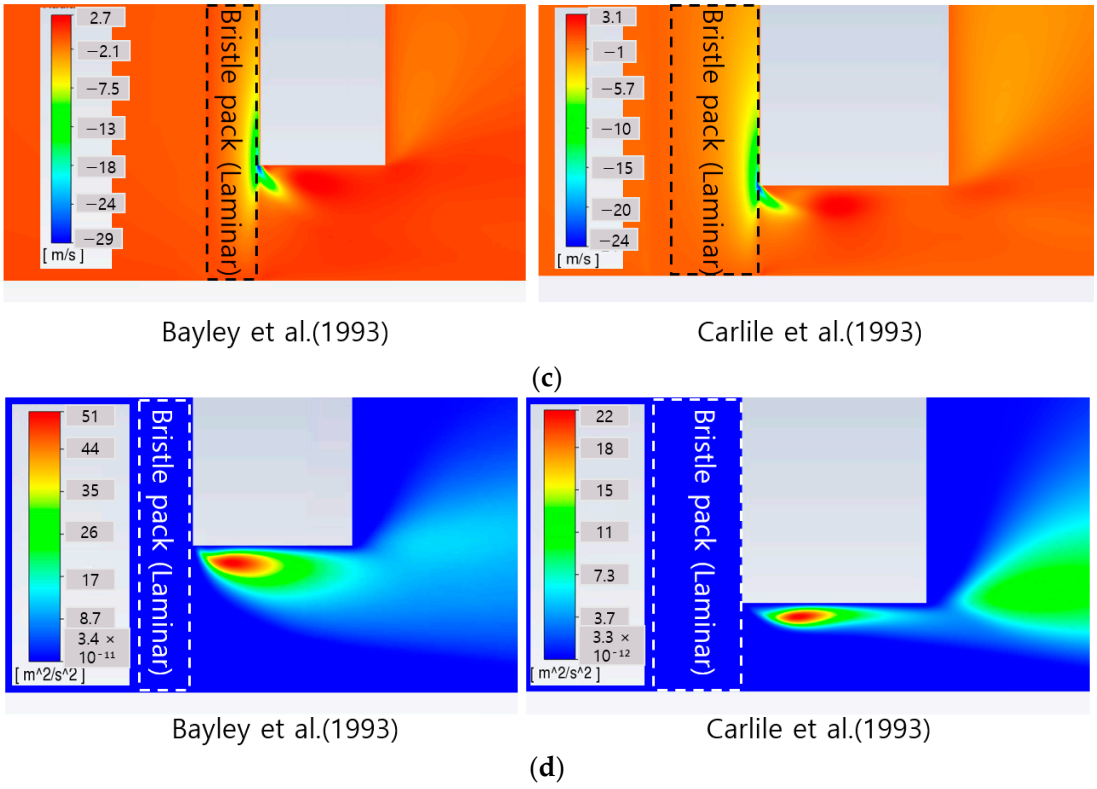

Figure 7. Flow fields around contact brush seals obtained via 2D CFD under a pressure ratio of 2.0 using the geometries from Bayley et al. [25] (left) and Carlile et al. [26] (right); (**a**) pressure; (**b**) axial velocity; (**c**) radial velocity; (**d**) turbulent kinetic energy.

In both studies, the axial velocity (Figure 7b) increased downstream as the flow passed through the bristle pack, highlighting a common trend of high-velocity regions being formed near the backing plate [51]. For the Bayley et al. [25] geometry, a distinct high-velocity region was observed immediately downstream of the bristle pack, with a more localized distribution relative to the Carlile et al. [26] geometry. Conversely, for the Carlile et al. [26] geometry, the high-velocity region was more broadly spread, but its intensity was less pronounced than in the Bayley et al. [25] geometry.

The changes in radial velocity (Figure 7c) also show a common trend between the two geometries, with fluctuations observed as the flow passed through the bristle pack and moved downstream. These changes in radial velocity are associated with pressure drops. For the Bayley et al. [25] geometry, the variation in radial velocity was more distinct and followed a more consistent pattern compared with that for the Carlile et al. [26] geometry.

For both geometries, the turbulent kinetic energy (Figure 7d) reached its maximum value beneath the backing plate and gradually decreased as the fluid passed through the bristle pack [5]. However, for the Bayley et al. [25] geometry, the turbulent kinetic energy had a slightly higher maximum value and a more localized distribution compared with that for the Carlile et al. [26] geometry. In the Carlile et al. [26] geometry, the smaller bristle diameter and higher bristle density contributed to an overall reduction in the turbulent kinetic energy, however, these geometric characteristics also induced significant flow acceleration downstream of the backing plate. This acceleration led to the formation of shear layers, resulting in a localized increase in the turbulent kinetic energy in this region. Consequently, despite the generally lower turbulence levels in the Carlile et al. [26] geometry, the sharp velocity gradients downstream of the backing plate caused a pronounced rise in the turbulent kinetic energy, highlighting the impact of the flow dynamics specific to this geometry.

3.3. Simulation of Brush Seal with Clearance

For the brush seal with clearance, 2D CFD simulations were performed using the Turner et al. [27] geometry. The flow conditions and geometrical parameters are listed in Table 3. Moreover, the bristle density is known to be determined by the bristle diameter [20]. Therefore, since the bristle diameter of the Turner et al. [27] geometry is very similar to that of the Bayley et al. [25] geometry, the same bristle density of 94.5 per mm was used to calculate the porosity for the Turner et al. geometry [27].

Table 3. Flow conditions and geometrical parameters of brush seals with clearance [27].

Parameter	Turner et al. [27]
Bristle diameter (d)	0.076 mm
Bristle pack thickness (t)	0.75 mm
Bristle lay angle (ϕ)	45°
Fence height (H)	1.4 mm
Clearance (CL)	0.27 mm, 0.75 mm
Bristle density (N)	94.5 per mm
Upstream temperature	293.15 K
Downstream pressure	100 kPa
Pressure ratio $\left(\frac{p_u}{p_d}\right)$	1.07–3.8
Porosity (ε)	0.192

In brush seals with clearances, the blow-down effect, whereby the bristle pack moves toward the rotor, must be considered as it significantly impacts the flow. Therefore, the calculations were performed after setting the blow-down clearance for each pressure ratio based on the findings of Dogu et al. [52], who analyzed the blow-down effect in the Turner et al. [27] geometry using 2D axisymmetric CFD. The blow-down clearance is calculated by subtracting the extent of the blow-down from the initial clearance, as shown in Equation (5). The blow-down clearance for each clearance level is illustrated in Figure 8. As in the case without clearance, the flow resistance in the upper region was set 20% higher than that in the fence height region to match the experimental data [52].

$$Blow-down\ Clearance = Initial\ Clearance - (Blow-down). \quad (5)$$

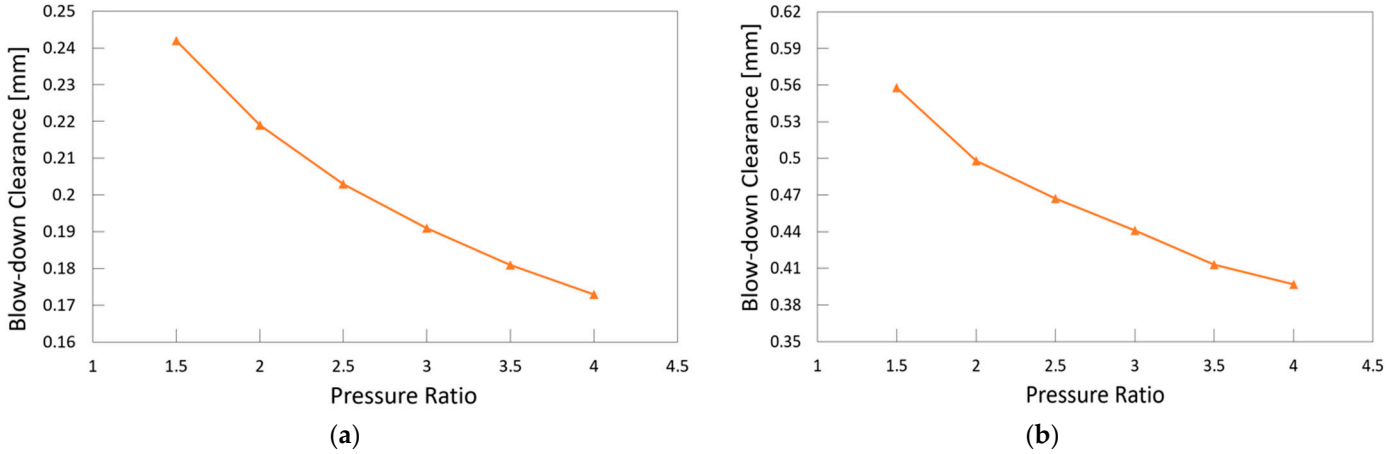

Figure 8. Variation in blow-down clearance with pressure ratio for different initial clearances: (**a**) clearance = 0.27 mm; (**b**) clearance = 0.75 mm.

As shown in Figure 9, the leakage flow rates were accurately predicted for the two clearance levels in the brush seals. Leakage flow rates were calculated using Equation (1), regardless of the blow-down clearance levels. When disregarding the blow-down effect, the leakage flow rate tends to be overestimated relative to the experimental data under high-

pressure conditions. Even a slight reduction in clearance results in a significant reduction in leakage [52].

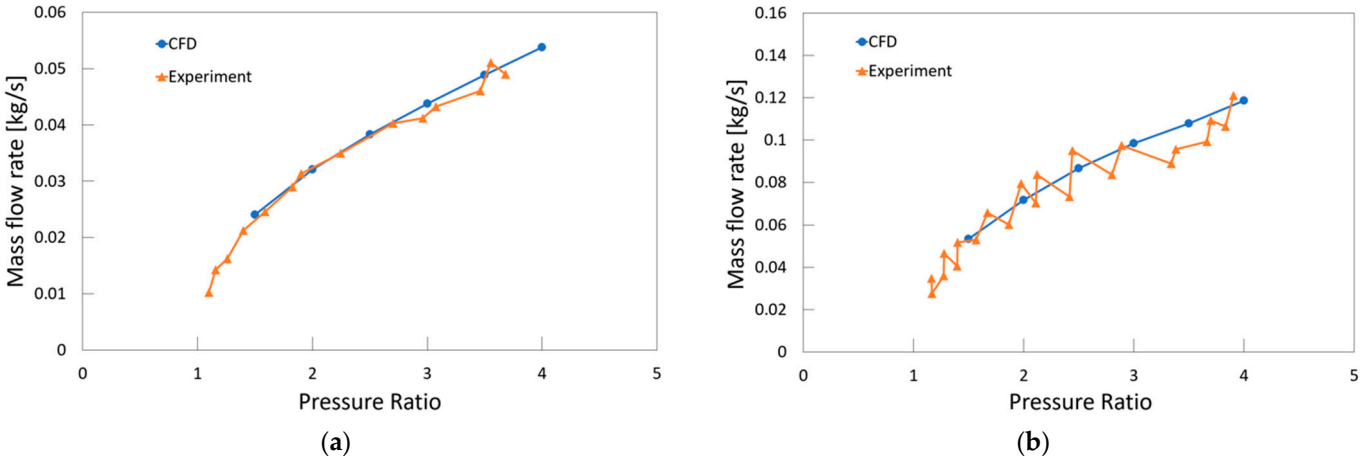

Figure 9. 2D CFD prediction of leakage flow rate in a brush seal considering blow-down clearance: (**a**) clearance = 0.27 mm; (**b**) clearance = 0.75 mm.

The CFD predictions for the brush seal with clearances are presented in Figure 10, and the observations are compared with those for the brush seals without clearance (Figure 7). Specifically, a comparison between the pressure distributions in Figures 7a and 10a reveals that in the case without clearance, the pressure was more uniformly maintained as the flow passed through the bristle pack, and the pressure drop in the downstream region was less abrupt. Contrarily, in the brush seal with clearances, the pressure drop was distributed across the thickness of the bristle pack, including the clearance, and it became more abrupt from upstream to downstream.

A comparison between the axial velocities in Figures 7b and 10b shows that in the case without clearance, the axial velocity remained relatively constant as the flow passed through the bristle pack, showing a more stable and consistent pattern. However, in the case with clearances, the axial velocity increased as the flow passed through the clearance, specifically at the clearance exit.

The radial velocity is also compared between Figures 7c and 10c. In the case without clearance, the radial velocity remained relatively constant as the fluid passed through the bristle pack, resulting in a less intense radial flow. By contrast, in the case with clearances, a strong radial flow was observed at the clearance inlet.

A comparison between the turbulent kinetic energies in Figures 7d and 10d, shows that, in the case without clearance, the turbulent kinetic energy was more evenly distributed within the bristle pack, with a lower maximum value and a broader distribution. However, in the case with clearances, a higher peak value was observed in the high-velocity region, and this peak occurred near the clearance.

Figure 11 compares the velocity vectors between the contact brush seal [25] and the brush seal with the 0.27 mm clearance [27], revealing distinct differences in flow behavior. For the contact seal, the flow predominantly diffused into the bristle pack, creating strong inward radial flow near the backing plate, which resulted in lower leakage rates. Conversely, for the seal with clearance, a significant portion of the flow bypassed the bristle pack through the clearance, leading to substantially higher leakage.

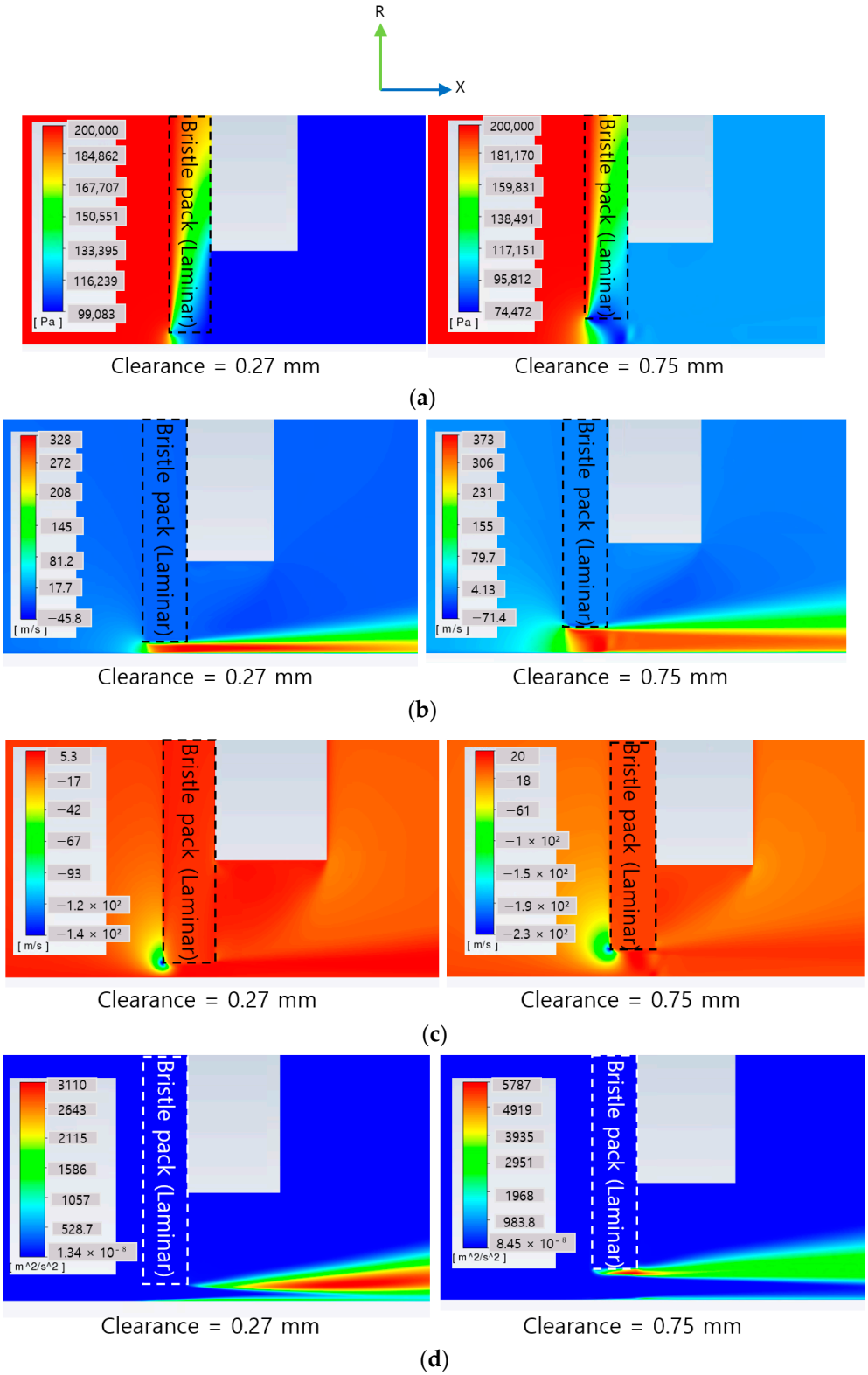

Figure 10. 2D CFD predictions of flow fields around brush seals with clearance under a pressure ratio of 2.0: (**a**) pressure; (**b**) axial velocity; (**c**) radial velocity; (**d**) turbulent kinetic energy.

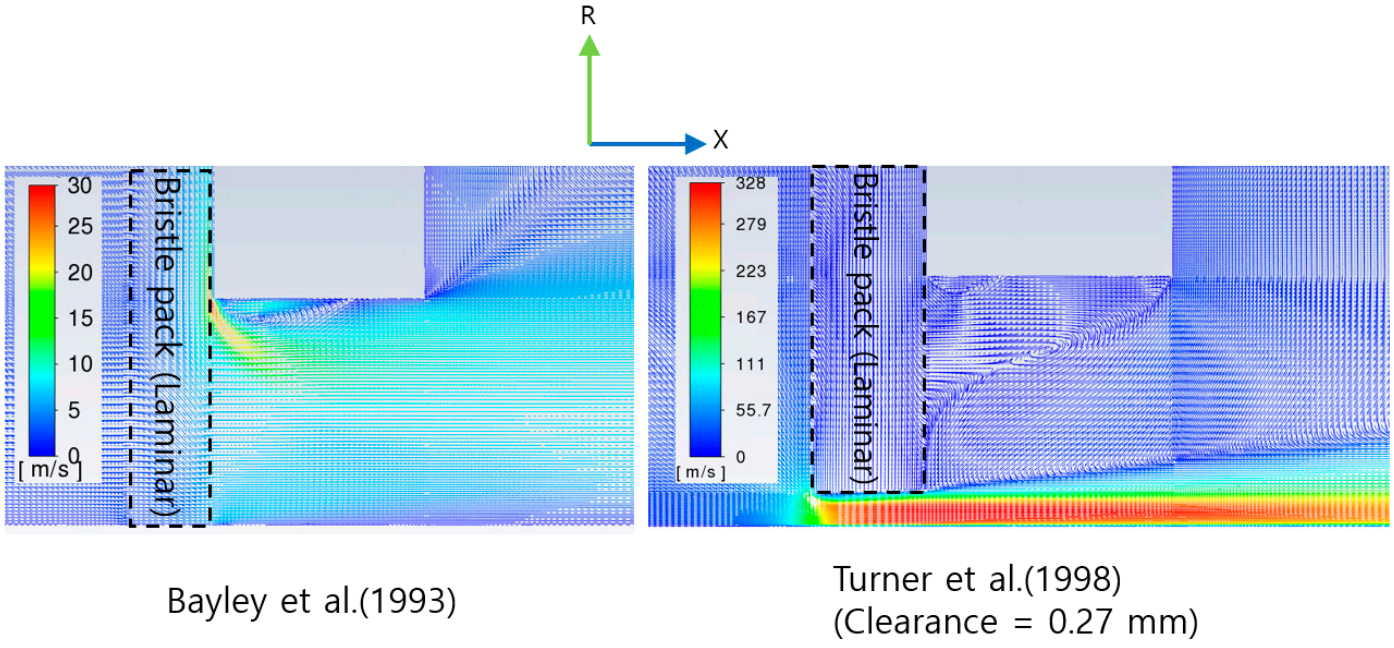

Figure 11. Velocity vectors around the fence height for contact [25] and clearance (0.27 mm) [27] brush seals under a pressure ratio of 2.0.

3.4. Blow-Down Prediction

Crudgington et al. [53] proposed a formula for calculating the blow-down effect. However, this formula is not universally applicable to brush seals with clearances and could not be employed under the conditions used to analyze the Turner et al. [27] geometry. Therefore, we developed a new blow-down formula specifically for the Turner et al. [27] geometry, based on the concept of effective clearance [48] utilized by Crudgington et al. [53]. Effective clearance is useful for accurately predicting and modeling the performance of brush seals and assists in controlling leakage flow in complex fluid dynamics environments such as turbines [54]. The blow-down formula proposed by Crudgington et al. [53] is challenging to use because it is tailored to a specific experimental setup involving a particular brush seal configuration and clearance geometry. The lack of a clear specification for the effective clearance further complicates the application of this formula. The formula accounts for factors such as bristle pack dynamics, pressure distribution, and axial compression, which differ significantly from the conditions employed by Turner et al. [27], where different pressure ratios and clearance conditions result in varying blow-down behaviors. To address these issues, a new calculation formula was developed to determine the blow-down, based on the effective clearance suggested by Zhang et al. [48]. This effective clearance is calculated using Equations (6) and (7), where γ and R are set to 1.4 and 287 J/kg·K, respectively, based on the properties of air. Q is a flow function that accounts for the compressibility and flow characteristics of the fluid, as expressed in Equation (7).

$$h_{eff} = \dot{m}\sqrt{T_u}/(\pi d_1 p_u Q), \tag{6}$$

$$Q = \begin{cases} \sqrt{\frac{2\gamma}{R(\gamma-1)}\left[\left(\frac{p_d}{p_u}\right)^{\frac{2}{\gamma}} - \left(\frac{p_d}{p_u}\right)^{\frac{\gamma+1}{\gamma}}\right]}, & \text{if } \frac{p_u}{p_d} \le \left(\frac{\gamma+1}{2}\right)^{\frac{\gamma}{\gamma-1}} \\ \sqrt{\frac{\gamma}{R}\left(\frac{2}{\gamma+1}\right)^{\frac{\gamma+1}{\gamma-1}}}, & \text{if } \frac{p_u}{p_d} \ge \left(\frac{\gamma+1}{2}\right)^{\frac{\gamma}{\gamma-1}} \end{cases}. \tag{7}$$

Following the methodology of Crudgington et al. [53], the effective clearance was calculated for both the non-blow-down state and the contact state. Additionally, the increase in blow-down with increasing pressure ratio was accounted for. Since the final calculated blow-down is in millimeters, the blow-down clearance can be obtained by subtracting the

blow-down value from the initial clearance. The blow-down calculation formula used for the Turner et al. [27] geometry is shown in Equation (8):

$$Blow-down = \frac{h_{eff}1 - h_{eff}2}{\left(\frac{CL}{d}\right)^{0.21}} - \frac{CL}{\left(\frac{CL}{d}\right)^{\frac{PR}{2}}}. \quad (8)$$

In Equation (8), $h_{eff}1$ represents the effective clearance calculated using the mass flow rate considering the initial clearance, without blow-down, and $h_{eff}2$ represents the effective clearance calculated using the mass flow rate in the contact state, without clearance. The formula is designed to account for variations in blow-down depending on the clearance level. Using Equation (8), the blow-down clearance and leakage flow for the Turner et al. [27] geometry were determined and were compared with the values reported by Dogu et al. [52], as shown in Figures 12 and 13. Based on the comparison, the maximum relative error was 4.8%, which occurred at a pressure ratio of 1.5 and a clearance of 0.75 mm. Therefore, Equation (8) can accurately predict the blow-down behavior for the Turner et al. [27] geometry.

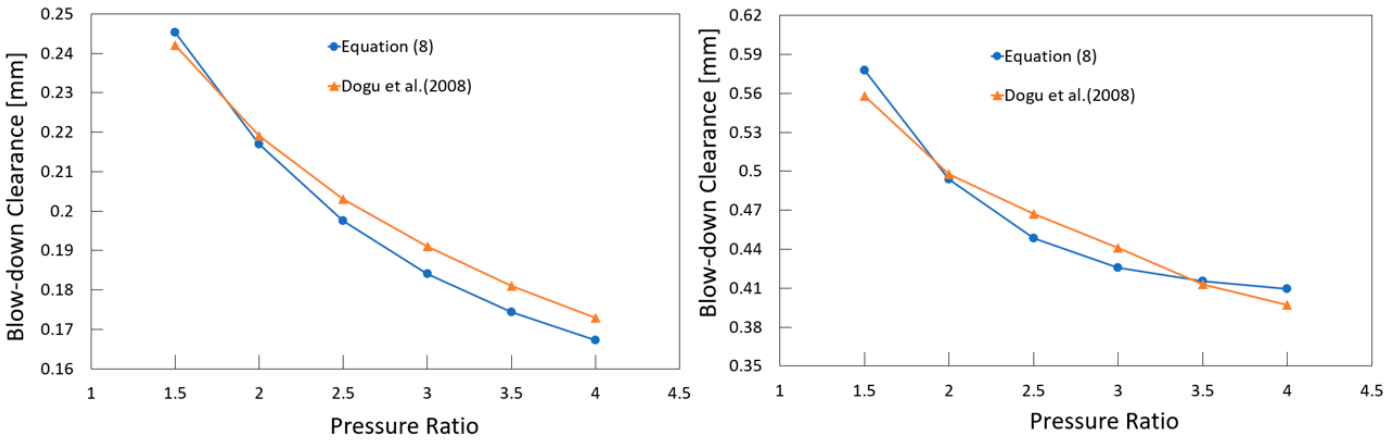

Figure 12. Comparison of predicted blow-down clearance (Equation (8)) with simulation results reported by Dogu et al. [52]: (**a**) clearance = 0.27 mm; (**b**) clearance = 0.75 mm.

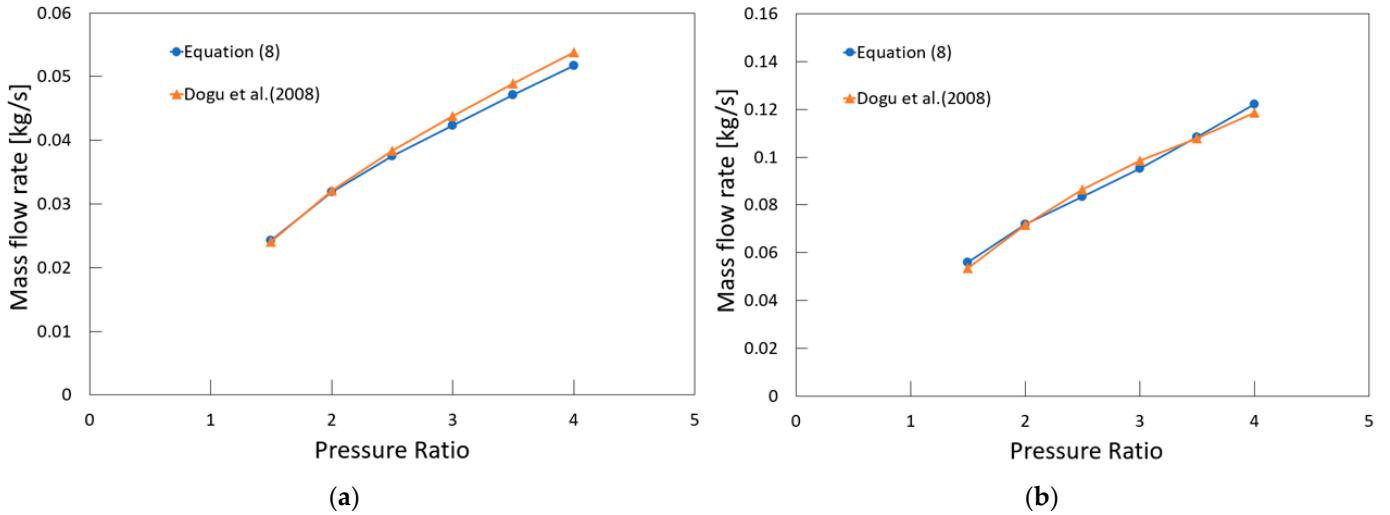

Figure 13. Comparison of leakage flow rate considering blow-down clearance between Equation (8) and simulation data [52]: (**a**) clearance = 0.27 mm; (**b**) clearance = 0.75 mm.

4. Conclusions

In this study, we modeled the bristles in a brush seal as a porous medium and conducted 2D CFD simulations. When the porosity is set based solely on static geometrical values, the leakage flow rate tends to be underestimated. To address this, we adjusted the porosity value to achieve accurate prediction with respect to experimental data. Additionally, we developed and validated an equation that predicts the blow-down effect for a brush seal with a clearance, without the need for FSI analysis. The key conclusions from this study are as follows:

The leakage flow rate of a brush seal in the contact state could be accurately predicted within a pressure ratio range of 1.5–6 by correcting the porosity based on the geometry and pressure ratio. By implementing the flow resistance derived from the corrected porosity, the leakage flow rate can be predicted with more than twice the accuracy (in terms of R^2) compared with standard 2D CFD simulations.

For a brush seal with a clearance in the blow-down state, the leakage flow rate could be predicted accurately using the developed porosity correction coefficient. Observations from the 2D CFD flow field indicated that in the presence of a clearance, the pressure drop occurs more rapidly, and changes in both the axial and radial velocities are more pronounced. The maximum turbulence kinetic energy is observed near the clearance.

In the case of a brush seal with a clearance, even without accounting for bristle bending, the leakage flow rate could be predicted with appropriate accuracy through 2D CFD simulations by considering the blow-down clearance. When the pressure ratio ranged between 1.5 and 4.0, the relative error between the leakage flow rates measured for the Turner et al. geometry [27] and those calculated using the proposed formula remained below 5%.

The main advantage of this formula lies in the accuracy of the predictions, with the relative error being less than 5% even without the use of FSI analysis. The porosity correction factor and blow-down calculation formula developed in this study represent significant advancements in brush seal design. Compared with previous research [23], the use of 2D CFD simulations in this study represents a more efficient and cost-effective approach for predicting leakage flow rates. However, the limitations of 2D simulations must also be considered as they cannot fully capture the 3D effects and complex FSIs involved in real-world applications.

Author Contributions: J.W.K. carried out the simulations, analyzed the CFD data, and wrote the paper. J.A. supervised the research, analyzed the CFD data, and wrote the paper. All authors have read and agreed to the published version of the manuscript.

Funding: This work was supported by the Agency for Defense Development Grant funded by the Korean Government (UD220004JD).

Institutional Review Board Statement: Not applicable.

Informed Consent Statement: Not applicable.

Data Availability Statement: The original contributions presented in the study are included in the article, further inquiries can be directed to the corresponding author.

Conflicts of Interest: The authors declare no conflicts of interest.

Nomenclature

$\dot{m}$	Mass flow rate [kg/s]
$\vec{u}$	Velocity vector of the fluid [m/s]
dA	Differential area vector [m^2]
d	Bristle diameter [mm]
d_I	Rotor diameter [m]
t	Bristle pack thickness [mm]
C	Viscous resistance constant [$1/m^2$]

D	Inertial resistance constant [1/m]
a_n	Viscous resistance coefficient in the direction normal to the bristles [1/m^2]
a_s	Viscous resistance coefficient in the lengthwise direction of the bristles [1/m^2]
b_n	Inertial resistance coefficient in the direction normal to the bristles [1/m]
b_s	Inertial resistance coefficient in the lengthwise direction of the bristles [1/m]
H	Fence height [mm]
PR	Pressure ratio $\left(\frac{p_u}{p_d}\right)$
CL	Clearance [mm]
N	Bristle density [1/mm]
T	Temperature [K]
Q	Flow function [s·K$^{0.5}$/m]
p	Pressure [kPa]
R	Specific gas constant [J/kg·K]
h_{eff}	Effective clearance [mm]
FSI	Fluid–structure interaction
X	Axial co-ordinate
R	Radial co-ordinate
Greek Symbols	
θ	Circumferential co-ordinate
γ	Isentropic coefficient
ϕ	Bristle Lay angle [°]
ε	Porosity
α	Porosity correction factor
ρ	Fluid density [kg/m^3]
Subscripts	
u	Upstream
d	Downstream

References

1. Boyce, M.P. *Gas Turbine Engineering Handbook*; Elsevier: Amsterdam, The Netherlands, 2011.
2. Goldstein, R.J.; Eckert, E.R.G.; Ramsey, J.W. Film cooling with injection through Holes: Adiabatic wall temperatures down-394 stream of a circular hole. *J. Eng. Power* **1968**, *90*, 384–393. [CrossRef]
3. Ahn, J.; Song, J.C.; Lee, J.S. Fully coupled large eddy simulation of conjugate heat transfer in a ribbed channel with a 0.1 blockage ratio. *Energies* **2021**, *14*, 2096. [CrossRef]
4. Pugachev, A.O.; Michael, D. Experimental and theoretical rotordynamic stiffness coefficients for a three-stage brush seal. *Mech. Syst. Signal Process.* **2012**, *31*, 143–154. [CrossRef]
5. Dogu, Y. Investigation of brush seal flow characteristics using bulk porous medium approach. *J. Eng. Gas Turbines Power* **2005**, *127*, 136–144. [CrossRef]
6. Yue, C.; Bitian, S.; Lanzhu, Z. Leakage performance predictions of a brush seal based on fluid–solid coupling method. *Sci. Prog.* **2020**, *103*, 1–17. [CrossRef] [PubMed]
7. Chupp, R.E.; Hendricks, R.C.; Lattime, S.B.; Steinetz, B.M.; Aksit, M.F. Turbomachinery clearance control. In *Turbine Aerodynamics, Heat Transfer, Materials, and Mechanics*; American Institute of Aeronautics and Astronautics, Inc.: Reston, VA, USA, 2014; pp. 61–188.
8. Schwarz, H.; Friedrichs, J.; Flegler, J. Axial inclination of the bristle pack, a new design parameter of brush seals for improved operational behavior in Steam turbines. *Turbo Expo Power Land Sea Air* **2014**, *1B*, V01BT27A036.
9. Bowsher, A.; Crudgington, P.; Kirk, T.; Chupp, R. Aspects of Brush Seal Design. In Proceedings of the 51st AIAA/SAE/ASEE Joint Propulsion Conference, Orlando, FL, USA, 27–29 July 2015; p. 4230.
10. Mehta, J.; Holloway, G.; Rosado, L.; Doak, D.; Hubley, C.; Askew, J.; Krawiecki, S. Innovative Rotating Intershaft Brush Seal for Sealing between Rotating Shafts Part II: Modeling of the Brush Seal Leakage Flows. In Proceedings of the 42nd AIAA/ASME/SAE/ASEE Joint Propulsion Conference & Exhibit, Sacramento, CA, USA, 9–12 July 2006; p. 4752.
11. Liu, Y.; Dong, W.; Chew, J.; Pekris, M.; Yue, B.; Kong, X. Flow conditioning to control the effects of inlet swirl on brush seal performance in gas turbine engines. *Front. Energy Res.* **2022**, *9*, 815152. [CrossRef]
12. Neef, M.; Sulda, E.; Sürken, N.; Walkenhorst, J. Design features and performance details of brush seals for turbine applications. *Turbo Expo Power Land Sea Air* **2006**, *4238*, 1385–1392.
13. Pekris, M.J.; Gervas, F.; David, R.G. An investigation of flow, mechanical, and thermal performance of conventional and pressure-balanced brush seals. *J. Eng. Gas Turbines Power* **2014**, *136*, 062502. [CrossRef]
14. Wei, Y.; Ran, X.; Xiong, B.; Liu, S. Influence of brush seal hysteresis effect on the nonlinear characteristics of rotor system. *Commun. Nonlinear Sci. Numer. Simul.* **2023**, *121*, 107239. [CrossRef]

15. Cieślewicz, S.M. *CFD-Simulations for Advanced Turbomachinery Sealing Technologies: Brush Seals*; Vienna University of Technology: Vienna, Austria, 2004.
16. Dogu, Y.; Sertcakan, M.C.; Gezer, K.; Kocagul, M. Flow resistance coefficients of porous brush seal as a function of pressure load. *J. Eng. Gas Turbines Power* **2018**, *140*, 082504. [CrossRef]
17. Song, X.; Liu, M.; Yang, J. Numerical analysis of leakage performance of brush seal based on a 2-d tube bank model and porous medium model considering the effect of compressible gas. *Int. J. Fluid Mach. Syst.* **2022**, *15*, 329–343. [CrossRef]
18. Hu, Y.; Chen, W.; Li, P.; Li, N.; Zhou, K.; Pan, J. Experimental investigation on the influence of bristle lay angle on the leakage characteristics of low hysteresis brush seals. *AIP Adv.* **2021**, *11*, 085012. [CrossRef]
19. Ahmed, A.A.M.; Liu, M.; Kang, Y.; Wang, J.; Idriss, A.I.B.; Tin, N.T.T. Brush seal performance with ideal gas working fluid under static rotor condition. *Machines* **2024**, *12*, 476. [CrossRef]
20. Aksit, M.F. *Brush Seals and Common Issues in Brush Seal Applications*; NATO: Brussels, Belgium, 2012.
21. Bowen, J.P.; Bowsher, A.A.; Crudgington, P.F.; Bull, S.; Sangan, C.M.; Scobie, J.A. Tracking of bristle tip deflections to demonstrate blow-down in brush seals. *Turbo Expo Power Land Sea Air* **2024**, *88001*, V008T14A020.
22. Bahadori, M.; Zirak, S. Effect of a ring type barrier and rotational speed on leakage flow of gas turbine brush seal. *Energy Equip. Syst.* **2019**, *7*, 389–399.
23. Kwon, J.W.; Ahn, J. Evaluation of gas turbine brush seal performance using a one-dimensional code. *Trans. Korean Soc. Mech. Eng. B* **2024**, *48*, 589–598. [CrossRef]
24. Lee, J.J.; Kang, S.Y.; Kim, T.S.; Byun, S.S. Thermo-economic analysis on the impact of improving inter-stage packing seals in a 500 MW class supercritical steam turbine power plant. *Appl. Therm. Eng.* **2017**, *121*, 974–983. [CrossRef]
25. Bayley, F.J.; Long, C.A. A combined experimental and theoretical study of flow and pressure distributions in a brush seal. *J. Eng. Gas Turbines Power* **1993**, *115*, 404–410. [CrossRef]
26. Carlile, J.A.; Hendrics, R.C.; Yoder, D.A. Brush seal leakage performance with gaseous working fluids at static and low rotor speed conditions. *J. Eng. Gas Turbines Power* **1993**, *115*, 397–403. [CrossRef]
27. Turner, M.T.; Chew, J.W.; Long, C.A. Experimental investigation and mathematical modeling of clearance brush seals. *J. Eng. Gas Turbines Power* **1998**, *120*, 573–579. [CrossRef]
28. Zhang, Y.; Li, J.; Yan, X.; Li, Z. Experimental and numerical investigations on leakage flow characteristics of two kinds of brush seals. *Turbo Expo Power Land Sea Air* **2018**, *51098*, V05BT15A026.
29. Sun, D.; Liu, N.N.; Fei, C.W.; Hu, G.Y.; Ai, Y.T.; Choy, Y.S. Theoretical and numerical investigation on the leakage characteristics of brush seals based on fluid–structure interaction. *Aerosp. Sci. Technol.* **2016**, *58*, 207–216. [CrossRef]
30. Kvamsdal, T.; Jenssen, C.; Okstad, K.; Amundsen, J. Fluid-structure interaction for structural design. In *Proceedings of the International Symposium on Computational Methods for Fluid-Structure Interaction (FSI'99)*; Tapir Publishers: Trondheim, Norway, 1999; pp. 211–238.
31. Li, J.; Qiu, B.; Jiang, S.; Kong, X.; Feng, Z. Experimental and numerical investigations on the leakage flow characteristics of the labyrinth brush seal. *Turbo Expo Power Land Sea Air* **2012**, *44700*, 2201–2210.
32. Abbas, A.M.; Pekris, M.J.; Chew, J.W. Investigation of grooved front plate for inlet swirl reduction in brush seals. *Turbo Expo Power Land Sea Air* **2024**, *88001*, V008T14A015.
33. Huang, S.Q.; Suo, S.F.; Du, K.B.; Li, Y.J.; Wang, Y.M. Study on a type of low-leakage brush seal porous media model. *Appl. Mech. Mater.* **2013**, *312*, 345–349. [CrossRef]
34. Germen, M. *Porous Medium Flow Simulation in a Brush Seal with Radial Clearance*; Vienna University of Technology: Vienna, Austria, 2012.
35. Görgün, E. A Study of Porous Media Resistance Coefficients for Brush Seals. Ph.D. Thesis, Sabancı University, Tuzla, Türkiye, Sabanci University, Istanbul, Turkey, 2014.
36. Qiu, B.; Li, J.; Feng, Z. Investigation of conjugate heat transfer in brush seals using porous media approach under local thermal non-equilibrium conditions. *Turbo Expo Power Land Sea Air* **2015**, *56734*, V05CT15A009.
37. Li, J.; Huang, Y.; Li, Z.; Feng, Z.; Yang, H.; Yang, J.; Shi, L. Effects of clearances on the leakage flow characteristics of two kinds of brush seals and referenced labyrinth seal. *Turbo Expo Power Land Sea Air* **2010**, *43994*, 1133–1142.
38. Park, D.S.; Ha, T.W. Rotordynamic characteristic analysis of brush seal using CFD. *KSFM J. Fluid Mach.* **2018**, *21*, 21–27. [CrossRef]
39. Song, X.; Liu, M.; Sun, J.; Wang, J.; Wang, K. Temperature field and performance analysis of brush seals based on FEA-CFD and the porous medium of anisotropic heat transfer models. *Energies* **2023**, *16*, 7306. [CrossRef]
40. Dogu, Y.; Bahar, A.S.; Sertçakan, M.C.; Pişkin, A.; Arıcan, E.; Kocagül, M. Computational fluid dynamics investigation of brush seal leakage performance depending on geometric dimensions and operating conditions. *J. Eng. Gas Turbines Power* **2016**, *138*, 032506. [CrossRef]
41. Varma, K.K.; Varma, B.S.; Kumari, K.R. CFD analysis of a heat exchanger using enhanced wall treatment function to capture the laminar sub-layer close to the wall. *Int. J. Mech. Eng. Res. Dev.* **2019**, *9*, 263–278.
42. Johnson, R.W. *Validation Studies for Numerical Simulations of Flow Phenomena Expected in the Lower Plenum of a Prismatic VHTR Reference Design*; Idaho National Lab.(INL): Idaho Falls, ID, USA, 2005.
43. Chun, Y.H.; Ahn, J. Optimizing the geometric parameters of a stepped labyrinth seal to minimize the discharge coefficient. *Processes* **2022**, *10*, 2019. [CrossRef]
44. Chew, J.W.; Hogg, S.I. Porosity modeling of brush seals. *J. Tribol.* **1997**, *119*, 769–775. [CrossRef]

45. Pröstler, S. Modellierung und numerische Berechnung von Wellenabdichtungen in Brstenbauart. Ph.D. Thesis, Ruhr-Universität, Bochum, Germany, 2005.
46. Pugachev, A.O.; Deckner, M. CFD prediction and test results of stiffness and damping coefficients for brush-labyrinth gas seals. *Turbo Expo Power Land Sea Air* **2010**, *44014*, 175–185.
47. Ma, D.; Li, Z.; Li, J. A three-dimensional tube bundle model analysis for leakage flow characteristics of variable bristle diameter brush seals with bristle pack stratification. *J. Eng. Gas Turbines Power* **2021**, *143*, 051014. [CrossRef]
48. Zhang, Y.; Dengqian, M.; Jun, L.; Yuan, H.; Jingjin, J.; Bo, S.; Zhigang, L.; Xin, Y. Effect of the fence height on the leakage flow characteristics of brush seals. *Glob. Power Propuls. Soc.* **2019**. [CrossRef]
49. Bowen, J.P.; Jenkins, M.R.; Bowsher, A.A.; Crudgington, P.F.; Sangan, C.M.; Scobie, J.A. The inter-bristle pressure field in a large-scale brush seal. *J. Eng. Gas Turbines Power* **2022**, *144*, 111022. [CrossRef]
50. Qiu, B.; Jun, L. Numerical investigations on the heat transfer behavior of brush seals using combined computational fluid dynamics and finite element method. *J. Heat Transfer* **2013**, *135*, 122601. [CrossRef]
51. Chen, L.H.; Wood, P.E.; Jones, T.V.; Chew, J.W. An iterative CFD and mechanical brush seal model and comparison with experimental results. *Turbo Expo Power Land Sea Air* **1998**, *78651*, V004T09A067.
52. Dogu, Y.; Aksit, M.F.; Demiroglu, M.; Dinc, O.S. Evaluation of flow behavior for clearance brush seals. *J. Eng. Gas Turbines Power* **2008**, *130*, 012507. [CrossRef]
53. Crudgington, P.; Bowsher, A. Brush seal blow down. In Proceedings of the 39th AIAA/ASME/SAE/ASEE Joint Propulsion Conference and Exhibit, Huntsville, AL, USA, 20–23 July 2003; p. 4697.
54. Jolly, P.; Arghir, M.; Bonneau, O.; Coirier, R.; Fiore, G. Experimental characterization of a two stage brush seals: Leakage and torque measurements. *Turbo Expo Power Land Sea Air* **2023**, *11A*, V11AT22A021.